

Drivers of the severity of the extreme hot summer of 2015 in western China

Article

Accepted Version

Chen, W. and Dong, B. ORCID: <https://orcid.org/0000-0003-0809-7911> (2018) Drivers of the severity of the extreme hot summer of 2015 in western China. *Journal of Meteorological Research*, 32 (6). pp. 1002-1010. ISSN 2198-0934 doi: 10.1007/s13351-018-8004-y Available at <https://centaur.reading.ac.uk/79536/>

It is advisable to refer to the publisher's version if you intend to cite from the work. See [Guidance on citing](#).

To link to this article DOI: <http://dx.doi.org/10.1007/s13351-018-8004-y>

Publisher: Springer

All outputs in CentAUR are protected by Intellectual Property Rights law, including copyright law. Copyright and IPR is retained by the creators or other copyright holders. Terms and conditions for use of this material are defined in the [End User Agreement](#).

www.reading.ac.uk/centaur

CentAUR

Central Archive at the University of Reading

Reading's research outputs online

Citation: Chen, W., B. Dong., 2018: Drivers of the extreme hot summer of 2015 in western China. *J. Meteor. Res.*, **32**(6), doi: 10.1007/s13351-018-8004-y.(in press)

Drivers of the Severity of the Extreme Hot Summer of 2015 in Western China

Wei CHEN^{1*} and Buwen DONG

1 LASG, Institute of Atmospheric Physics, Chinese Academy of Sciences, Beijing 100029, China

2 National Centre for Atmospheric Science–Climate, Department of Meteorology, University of Reading, Reading RG6 6AH, UK

(Received January 15, 2018; in final form August 28, 2018)

Supported by the National Natural Science Foundation of China (416750788, U1502233, 41320104007), the Youth Innovation Promotion Association of CAS (2018102), and the Natural Environment Research Council via the National Centre for Atmospheric Science

Corresponding author: chenwei@mail.iap.ac.cn.

©The Chinese Meteorological Society and Springer-Verlag Berlin Heidelberg 2018

ABSTRACT

Western China experienced an extreme hot summer in 2015, breaking a number of temperature records. The summer mean surface air temperature (SAT) anomaly was twice the interannual variability. The hottest daytime temperature (T_{Xx}) and warmest night-time temperature (T_{Nx}) were the highest in China since 1964. This extreme hot summer occurred in the context of steadily increasing temperatures in recent decades. We carried out a set of experiments to evaluate the extent to which the changes in sea surface temperature (SST)/sea ice extent (SIE) and anthropogenic forcing drove the severity of the extreme summer of 2015 in western China. Our results indicate that about 65–72% of the observed changes in the seasonal mean SAT and the daily maximum (T_{max}) and daily minimum (T_{min}) temperatures over western China resulted from changes in boundary forcings, including the SST/SIE and anthropogenic forcing. For the relative role of individual forcing, the direct impact of changes in anthropogenic forcing explain about 42% of the SAT warming and 60% (40%) of the increase in T_{Nx} and T_{min} (T_{Xx} and T_{max}) in the model response. The changes in SST/SIE contributed to the remaining surface warming and the increase in hot extremes, which are mainly the result of changes in the SST over the Pacific Ocean, where a super El Niño event occurred. Our study indicates a prominent role for the direct impact of anthropogenic forcing in the severity of the extreme hot summer in western China in 2015, although the changes in SST/SIE, as well as the internal variability of the atmosphere, also made a contribution.

Keywords: severity of temperature extremes, summer 2015, western China, anthropogenic forcing

1. Introduction

2015 was the hottest year globally in terms of the surface air temperature (SAT) since modern meteorological records began (WMO Press Conference, 25 November 2015). The SAT in China during 2015 broke all historical records and was the warmest year since the complete weather record has appeared (CMA, 2016). In particular, compared to the same period in history, the SAT and extreme temperature records were both broken over western China in summer (June, July and August) 2015. Some observational stations in Xinjiang and Yunnan provinces recorded historical extremes for the daily maximum temperature and the number of extreme hot days (CMA, 2016). Turpan station experienced its highest recorded maximum temperature of 47.5 °C on 24 July 2015, which occurred after nine consecutive hot days with maximum temperatures >45 °C from 16 July 2015 (Xinhua net, 24 July 2015).

The global increase in hot extremes is attributed to anthropogenic activity (Christidis et al., 2011; Seneviratne et al., 2012; Bindoff et al., 2013; King et al., 2015, 2016). On the regional scale, the combined influence of anthropogenic forcing and natural atmospheric variability can be detected in temperature extremes over many land areas (Zwiers et al., 2011; Zhou et al., 2016). Changes in anthropogenic forcing and sea surface temperatures (SSTs) explain two-thirds of the magnitude of the 2015 heatwave over central Europe (Dong et al., 2016a). Anthropogenic activities doubled the probability of the 2013 heatwave in central and eastern China (Ma et al., 2017).

An attribution study may help our understanding of how much anthropogenic climate change has contributed to the change in the risk (probability) or severity (magnitude) of observed events (e.g. Otto et al., 2012; Stott et al., 2013; Stott, 2016).

It is possible to estimate how factors such as anthropogenic activity modify the risk and contribute to the severity of events, although a specific extreme event cannot be attributed to a single reason. One extreme event can be considered ‘mostly natural’ in terms of the severity and ‘mostly anthropogenic’ in terms of the risk of occurrence, such as the 2010 Russian heatwave (e.g. Dole et al., 2011; Rahmstorf and Coumou, 2011). These are two complementary aspects of an event and are not mutually exclusive, but depend on what question is being asked in addressing the attribution of individual weather events to external drivers of climate.

Previous studies have attributed human influence to the risk of the extreme heat event over western China in 2015 (Miao et al., 2016; Sun et al., 2016). Such an extreme event can be increased three-fold due to anthropogenic influences (Miao et al., 2016). Sun et al. (2016) further confirmed that there was more than 90% chance for this increase to be at least three-and-a-half-fold. These studies focused on the risk of this kind of event, but ignored the severity of such extreme events. Severity is a crucial features of extreme hot events and is directly related to an increase in mortality (Kilbourne, 1997; Dáz et al. 2002). As a semi-arid region, western China has a shortage of water resources and extreme heat events may result in ecological crises.

We performed a set of numerical experiments to assess the extent to which

changes in the SST/sea ice extent (SIE) and anthropogenic forcing drove the severity of the extreme hot summer in western China in 2015 and to quantify the relative roles of individual forcing factors. The structure of the paper is as follows. Section 2 describes the data and design of the model experiment. The observed changes over western China in summer 2015 are discussed in Section 3. Section 4 presents the simulated changes in response to different forcings and quantitatively evaluates the relative role of individual forcings in the severity of the extreme hot summer in western China in 2015. The conclusion and discussion are presented in Section 5.

2. Data and methods

The observational data were extracted from records of the national climatological daily temperature from 1964 to 2015 at 165 stations in western China (west of 105° E). These station observations are reliable and are representative of the region because the warming signals and extreme hot events are on a large spatial scale, although the station density is poor in some areas. In addition to the observed summer mean SAT, some extreme temperatures indices, including T_{\max} (the daily maximum temperature), T_{\min} (the daily minimum temperature), the diurnal temperature range (DTR), T_{Xx} (the annual hottest daytime temperature) and T_{Nx} (the annual warmest night-time temperature) were obtained. Each index was calculated for each individual station and then the regional mean was calculated.

An atmospheric configuration of the Meteorological Office Hadley Centre Global Environment Model version 3 (HadGEM3-A) was used in this study (Hewitt et al.,

2011). This model has a horizontal resolution of 1.875° longitude by 1.25° latitude and 85 vertical levels. We performed a set of experiments to detect the relative contribution of changes in the SST/SIE and forcing by anthropogenic greenhouse gases (GHG) and anthropogenic aerosols (AA) over western China in the extreme hot summer of 2015. Each experiment had 25 ensemble members and we analysed the ensemble mean. The CONTROL experiment was performed for the period 1964–1993. Four other experiments (2015ALL, 2015SST, 2015SSTGHG and 2015SSTATL) were performed for the period November 2014 to October 2015 with different forcings (Table 1).

There were two preconditions in this study: (1) we assumed that the responses to different forcings were added linearly and (2) we considered the changes in the SST/SIE and anthropogenic forcing as independent factors. The influence of individual forcing components on the temperatures in summer 2015 was examined. These components included: all forcing (2015All–CONTROL), GHG and anthropogenic aerosols (2015All–2015SST), GHG only (2015SSTGHG–2015SST), anthropogenic aerosols only (2015All–2015SSTGHG), global SSTs (2015SST–CONTROL), Pacific SSTs only (2015SST–2015SSTATL) and Atlantic SSTs only (2015SSTATL–CONTROL). The same set of experiments was used in the attribute study of the 2015 summer European heatwave (Dong et al., 2016a).

Table 1. Summary of numerical experiments.

Experiment	Boundary conditions
CONTROL	Forced with monthly mean climatological SSTs and SIE averaged over

the period 1964–1993 using HadISST data (Rayner et al., 2003) and with anthropogenic greenhouse gas (GHG) concentrations averaged over the same period and anthropogenic aerosol (AA) emissions averaged over the period 1970–1993 (Lamarque et al., 2010)

2015ALL

Forced with monthly mean SSTs and SIE from November 2014 to October 2015 using HadISST data, with the GHG concentrations in 2014 (WMO 2015) and AA emissions for 2015 from RCP4.5 scenario (Lamarque et al., 2011)

2015SSTGHG

As 2015ALL, but with AA emissions the same as in the CONTROL experiment

2015SST

As 2015ALL, but with GHG concentrations and AA emissions the same as in the CONTROL experiment

2015SSTATL

As 2015SST, but with SSTs outside the Atlantic the same as in the CONTROL experiment

141 SIE, sea ice extent; SST, sea surface temperature.

142 **3. Observed changes over western China during summer**

143 **2015**

144 Figure 1a and 1b show the temporal evolution of the SAT and extreme
 145 temperature anomalies averaged over western China relative to the climatological
 146 average from 1964 to 1993. The SAT anomaly over western China in summer 2015
 147 was 1.13 °C, twice the interannual variability of the SAT anomaly (0.60 °C). The SAT
 148 warming in 2015 occurred in the context of steadily increasing temperatures in recent
 149 decades, with a linear trend of 0.34 °C/decade. Summer 2015 set the highest records
 150 for the temperature extremes T_{Xx} and T_{Nx} since 1964. The anomalous T_{Xx} and T_{Nx}
 151 values were even higher than those in summer 2010 when the highest summer mean
 152 SAT record was set. T_{Xx} and T_{Nx} were 2.32 and 2.13 °C higher than the 1964–1993
 153 mean and 3.01 and 2.92 standard deviations of the interannual variability (0.77 °C for

154 T_{XX} and $0.73\text{ }^{\circ}\text{C}$ for T_{NX}), respectively. The hot temperature extremes in 2015 also
155 occurred under an increasing trend of temperature extremes. The linear trends are
156 $0.20\text{ }^{\circ}\text{C/decade}$ for T_{XX} and $0.39\text{ }^{\circ}\text{C/decade}$ for T_{NX} .

157 The seasonal mean T_{\max} and T_{\min} in summer 2015 showed strong positive
158 anomalies 1.19 and $1.26\text{ }^{\circ}\text{C}$ higher than the 1964–1993 mean. The 2015 T_{\max} anomaly
159 was twice the interannual variability ($0.60\text{ }^{\circ}\text{C}$) and 50% higher than the 2014 anomaly.
160 Western China experienced five more summer days (the annual number of days when
161 $T_{\max} > 25\text{ }^{\circ}\text{C}$) and six more tropical nights (the annual number of days when
162 $T_{\min} > 20\text{ }^{\circ}\text{C}$) in 2015 relative to the 1964–1993 average. The DTR anomaly over
163 western China was negative because the magnitude of the summer mean T_{\min} anomaly
164 was stronger than that of the T_{\max} anomaly. The anomalous negative DTR not only
165 appeared in 2015, but also several times since the mid-1990s, when there was a rapid
166 increase in both the mean temperature and temperature extremes. This indicates that
167 the warming amplitude in T_{\min} is stronger than that in T_{\max} , although they are both in
168 the context of a steady increase.

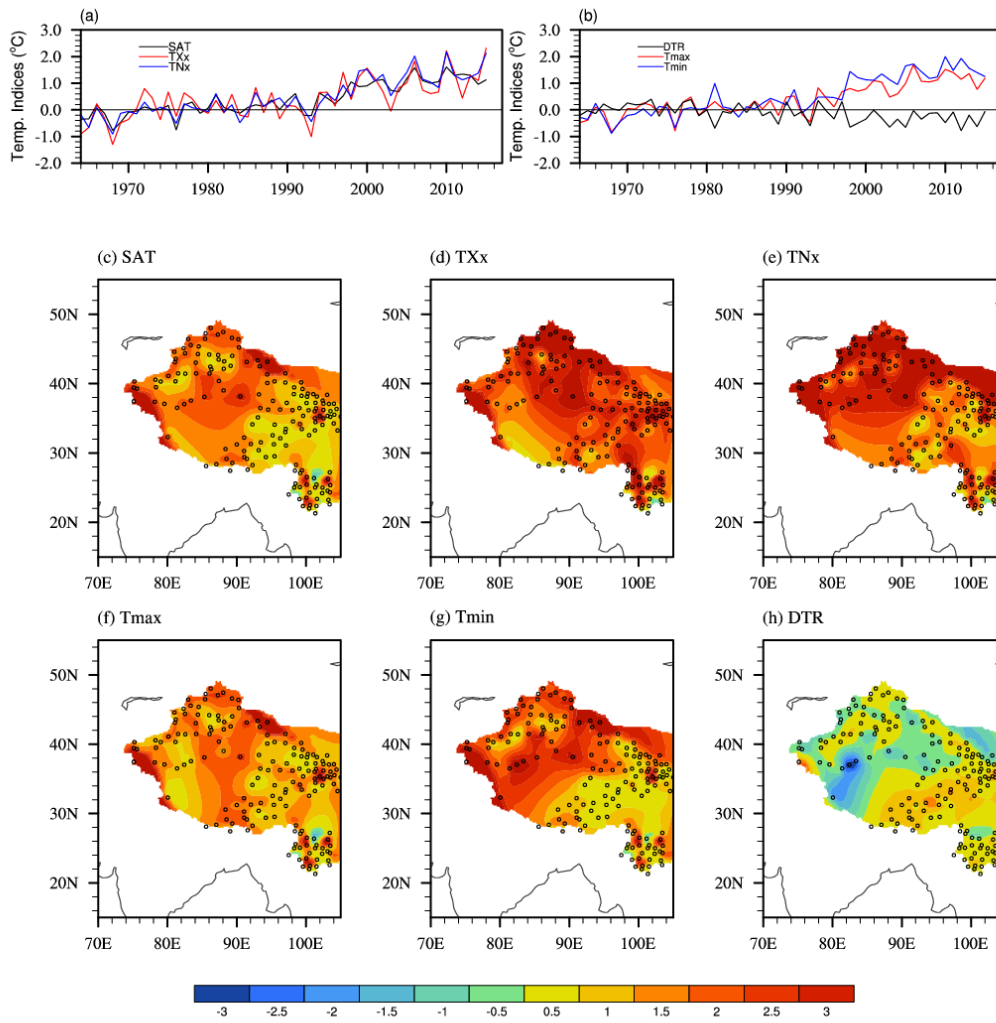


Fig. 1. (a, b) Time series of summer 2015 anomalies relative to the climatology (mean of 1964–1993 records) averaged over 165 stations in western China (west of 105° E) using the dataset of meteorological stations in China. (a) SAT, T_{XX} and T_{Nx} and (b) T_{max} , T_{min} and DTR. (c–h) Spatial patterns of 2015 anomalies relative to 1964–1993 for (c) the summer mean SAT, (d) T_{XX} , (e) T_{Nx} , (f) T_{max} , (g) T_{min} and (h) DTR from dataset of 165 meteorological stations in western China. Units: °C.

The SAT warming signal was observed over a large part of western China (Fig. 1c). The most significant warming was over central and the northern part of western China, where the anomalies were >3 °C. The maximum anomaly was >11 °C at Yiwu

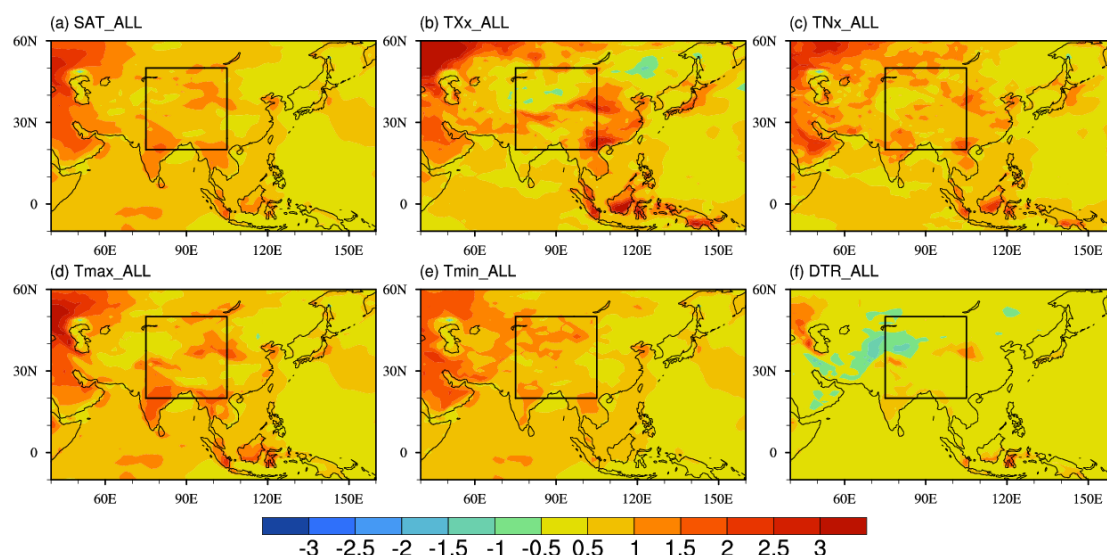
station (43.16 °N, 94.42 °E) in Xinjiang province. A remarkable increase in T_{Xx} and T_{Nx} was observed over western China (Fig. 1d and 1e). About 30% (20%) of the stations had a T_{Xx} (T_{Nx}) anomaly >3 °C above the climatology (46 stations for T_{Xx} and 36 stations for T_{Nx}). The spatial patterns for the T_{Xx} and T_{Nx} both showed a zonal gradient with a stronger increase in the northern part of western China than in the southern part. This similar distribution implies that regions with a higher hottest daytime temperature generally also had a higher warmest night-time temperature.

The seasonal mean T_{max} and T_{min} increased across all of western China (Fig. 1f and 1g). The most significant change for T_{max} was in central western China and the most significant change for T_{min} was in the northwestern part of western China. The magnitude of the T_{min} anomaly was marginally greater than that of the T_{max} anomaly, particularly in the northwest, where the negative DTR anomaly was observed (Fig. 2f). About 50% (88 stations) of the stations had a negative DTR anomaly.

4. Simulated changes in response to different forcings

The model response to changes in the SST/SIE and anthropogenic forcing (2015ALL) relative to the CONTROL experiment reproduced the general patterns of observed SAT warming and the hottest centre in the northern part of western China (Fig. 2a), although the simulated warming signal was more uniform than the observed results. The intensity of the SAT anomaly in response to all changes in forcing was weaker than the anomaly in the observed results, which implies either a deficiency in the model in response to changes in forcing or an effect from the internal variability

199 of atmosphere on the severity of the warming of the SAT in western China in summer
 200 2015.



201
 202 Fig. 2. Spatial patterns of changes in (a) the SAT, (b) T_{Xx} , (c) T_{Nx} , (d) T_{max} , (e) T_{min} and (f) DTR in
 203 response to all forcing changes (2015ALL-CONTROL). Units: $^{\circ}\text{C}$.

204 T_{Xx} and T_{Nx} in western China increased in response to all forcing changes,
 205 consistent with the observed results (Fig. 2b and 2c). The magnitude of the anomalies
 206 in T_{Xx} and T_{Nx} is underestimated by the simulation, particularly in the north of western
 207 China, but the simulated changes in T_{Xx} and T_{Nx} in south were close to those in the
 208 observations. These results imply a role of changes in the SST/SIE and anthropogenic
 209 forcing in the severity of T_{Xx} and T_{Nx} over western China, particularly over the
 210 southern part of western China.

211 The spatial distribution and intensity of the seasonal mean T_{max} and T_{min}
 212 anomalies were both well simulated by the model in response to all forcing changes
 213 (Fig. 2d and 2e). The negative DTR anomaly in the northwest of western China was

also captured by the model. This similarity indicates that changes in the SST/SIE and anthropogenic forcing played a dominant role in the severity of the summer mean T_{\max} and T_{\min} over western China in summer 2015.

Figure 3 shows a quantitative comparison of the changes in the mean SAT and temperature extremes over western China in summer 2015 between the observations and the simulated responses. The simulated changes in response to all forcing changes showed a warming SAT and an increase in temperature extremes, although with a weaker magnitude than the observed changes. The area-averaged summer SAT anomaly over western China in response to all forcing changes was 0.81 °C, about 72% of the observed anomaly. The area-averaged T_{\max} and T_{\min} anomalies were 0.79 and 0.82 °C, about 66.4 and 65.1% of the observed anomalies, respectively. These results indicate a dominant role of forcing changes, including the SST/SIE and anthropogenic forcing, in the observed summer warming and seasonal mean changes in T_{\max} and T_{\min} over western China in 2015.

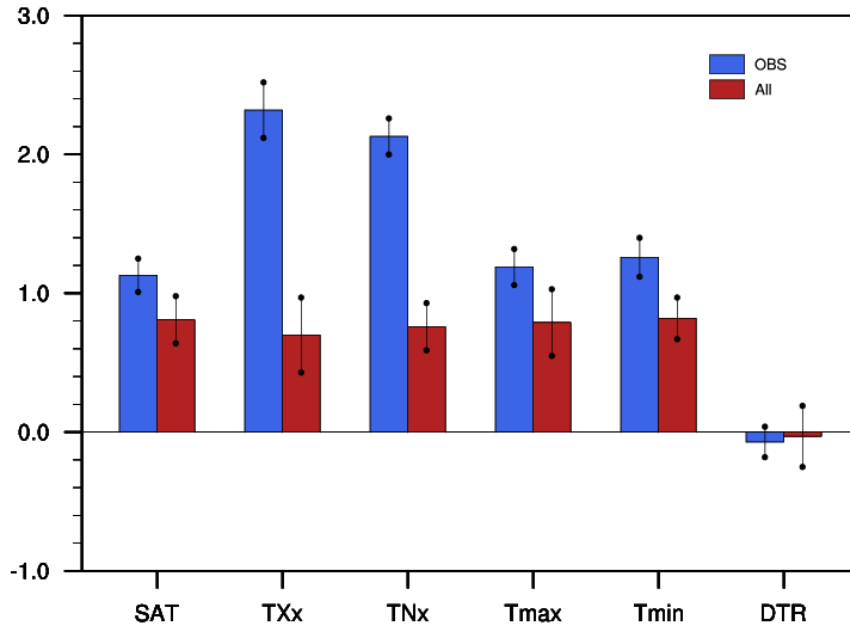


Fig. 3. Observed and simulated 2015 anomalies for SAT, T_{Xx} , T_{Nx} , T_{max} , T_{min} and DTR over western China (20–50° N, 75–105° E; masked by the Chinese border) in response to all forcing changes (2015ALL–CONTROL). The colour bar indicates the central estimates and the dots show the 90% confidence intervals based on the two-tailed Student's *t*-test. Units: °C.

The magnitude of T_{Xx} and T_{Nx} in the model responses to all forcing changes was clearly less than that in the observations. The area-averaged T_{Xx} (T_{Nx}) anomalies were about 30.2% (35.7%) of the observed increase in T_{Xx} (T_{Nx}). The underestimation of the mean response of the model in the magnitude of these hot temperature extremes (T_{Xx} and T_{Nx}) indicates the deficiency of the model in response to changes in external forcing. However, it also implies that the internal variability of the atmosphere might have played a part in the severity of the hot extremes in western China in 2015. The role of internal variability of the atmosphere will be discussed later in this paper.

Figure 4 shows the relative roles of different forcings in the severity of the extreme hot event over western China in 2015. The changes in SST/SIE play an

important part in the warming of the SAT and the increase in temperature extremes. The response of the SAT to changes in the SST/SIE is 0.47 °C, explaining 58.0% of the warming signal in the simulated SAT. For the temperature extremes, the responses to the changes in the SST/SIE were 0.45 °C for T_{Xx} and 0.57 °C for T_{max} , which were the most important contributing factors in the simulated increase in T_{Xx} and T_{max} (64.3% for T_{Xx} and 72.2% for T_{max}). The T_{Nx} and T_{min} response to changes in the SST/SIE were 0.30 and 0.36 °C, respectively, which represent 39.5 and 43.9% of the simulated changes. This result indicates that the role of changes in the SST/SIE in the magnitude of T_{Xx} and T_{max} was stronger than that in T_{Nx} and T_{min} .

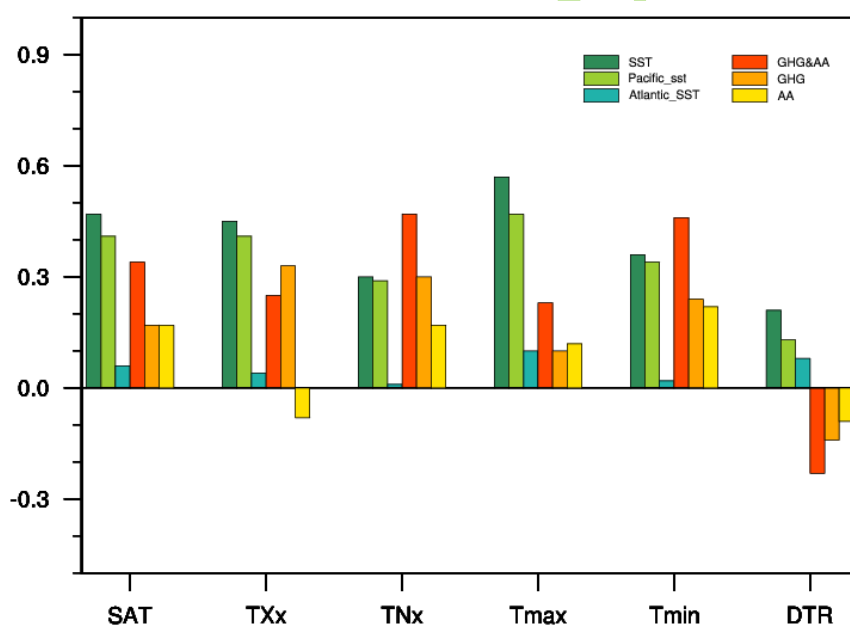


Fig. 4. Observed and simulated 2015 anomalies for SAT, T_{Xx} , T_{Nx} , T_{max} , T_{min} and DTR over western China (20–50° N, 75–105° E; masked by the Chinese border) in response to changes in individual forcings: SST/SIE, 2015SST–CONTROL; Pacific SST, 2015SST–2015SSTATL; Atlantic SST, 2015SSTATL–CONROL; GHG and anthropogenic aerosols (AA), 2015ALL–2015SST; GHG, 2015SSTGHG–2015SST; and AA, 2015ALL–2015SSTGHG. Units: °C.

The changes in SST/SIE mainly result from the changes in the SST over the Pacific Ocean, where a super El Niño event was developing in summer 2015. Therefore the increased temperature anomalies in response to the changes in SST/SIE were mainly to the south of 30° N (Supplementary Fig. S1), which were predominantly due to the warming effect related to the El Niño event.

The pattern of SST anomalies in summer 2015 suggested a prominent positive SST anomaly over the central and eastern tropical Pacific, which is known as the developing phase of the exceptionally strong 2015–2016 El Niño event (Supplementary Fig. S2a). The El Niño effect warms the tropical and subtropical regions, including the southern part of western China. The warming effect is manifested by a positive atmospheric thickness anomaly (the differences in geopotential height between 200 and 700 hPa) as a Kelvin wave response to strong warming over the central and eastern tropical Pacific (Supplementary Fig. S2b). This positive thickness anomaly corresponds to the anticyclonic circulation anomaly in the lower troposphere over western China (Supplementary Fig. S2c). The anomalous anticyclonic circulation favours an increase in downward solar radiation and warms the air mass by anomalous sinking, therefore contributing to the severity of the hot extremes, particularly the severity of daytime extremes (T_{xx} and T_{max}), over western China.

The responses to the direct impacts of changes in GHG and AA forcings explain the remaining magnitude of the simulated SAT warming and increase in temperature

extremes (Fig. 4 and Supplementary Fig. S3). Quantitatively, the additional changes of 42.0% in the SAT, 35.7% in T_{xx} , 27.8% in T_{max} , 60.5% in T_{Nx} and 56.1% in T_{min} were responses to the changes in anthropogenic forcing. In general, the effect of changes in GHG concentrations was stronger than that of changes in AA emissions, but they both led to a warming of the SAT and an increase in temperature extremes (except for a decrease in T_{xx} in response to changes in AA forcing). In particular, the responses of temperature extremes to changes in anthropogenic forcing were stronger at night (T_{Nx} and T_{min}) than during the day (T_{xx} and T_{max}). The larger changes in T_{min} than in T_{max} resulted in a negative DTR anomaly in response to forcing by GHG and AA forcing, which was in agreement with the observations, but with a stronger amplitude.

The warming induced over western China by AA forcing changes is due to remote changes in the emission of anthropogenic aerosols rather than local changes. Changes in AA emissions in 2015 suggest a reduction over Europe and North America and an increase over South and East Asia (Dong et al., 2016a). The local changes in AA emissions over western China were insignificant. The impacts of a decrease in AA emission over Europe led to local surface warming through aerosol–radiation and aerosol–cloud interactions. This warming extended downwards along the Eurasia continent and induced warming over western China by coupled land surface–atmosphere feedbacks as a result of drying of the land surface and reduced cloud cover, being consistent with the results of Dong et al. (2016b). Thus the surface

warming in summer and increases in the temperature extremes over western China were probably the result of the downstream extension of the climate response to reduced AA emissions over Europe (Supplementary Fig. S3).

The seasonal mean SAT and temperature extremes over western China for 1964–1993 and 2015 in both the observations and 25 realizations in the simulations are shown in Supplementary Fig. S4 to better illustrate the role of the forced response and internal atmospheric variability in the severity of the extreme hot summer of 2015. Basically, CONTROL experiment reproduces the interannual variability of the SAT and temperature extremes over western China in summer. The seasonal mean SAT, T_{Nx} and T_{min} are also in broad agreement with the observations. The biases are the underestimation of T_{max} , T_{Xx} and the DTR, which is a common bias in atmospheric general circulation models (AGCMS; e.g. Kysely and Plavcova, 2012; Cattiaux et al., 2015).

The 2015ALL and 2015SST experiments both intensify the seasonal mean SAT and temperature extremes relative to the CONTROL experiment, which suggests that anthropogenic forcing, as well as SST/SIE forcing, affects the severity of surface warming and the increase in temperature extremes in western China. The seasonal mean of T_{Xx} and T_{max} in 2015SST are close to those in 2015ALL, implying a dominant role of the changes in SST/SIE forcing in the simulated response of daytime extremes. The summer mean T_{Nx} and T_{min} in 2015ALL are clearly stronger than those in 2015SST, suggesting that changes in anthropogenic forcing are more effective in

increasing the severity of night-time temperature extremes.

Interestingly, several realizations in 2015ALL give a magnitude of SAT close to that in summer 2015 in the observations, but no such realization is seen in the CONTROL experiment and the 2015SST simulations (Supplementary Fig. S4a). This suggests that changes in anthropogenic forcing and the SST/SIE set preconditions for the severity of extremely hot SATs over western China, such as summer 2015, to occur in the model simulation. Several realizations in 2015ALL give magnitudes of the SAT and T_{\min} as strong as that in the summer 2015 observations (Supplementary Fig. S4a and S4e). One particular realization with the warmest T_{\min} and the second hottest SAT reproduces the severity of the extremely hot summer of 2015 over western China (Supplementary Figs S5 and S6). In this realization, the magnitude and spatial pattern of the SAT and temperature extremes were similar to those in the summer 2015 observations, suggesting a role for the internal variability of the atmosphere in the severity of the hot extremes over western China in summer 2015.

5. Discussion and conclusions

This study assessed the extent to which the severity of the extreme hot summer in western China in 2015 was forced by changes in the SST/SIE and forcings in GHG and AA emissions and quantified the relative role of individual forcing factors. The main findings can be summarized as follows.

- 1) Observations from meteorological stations in China indicate an extreme hot summer over western China in 2015 (165 stations west of 105 °E). The area-averaged

SAT anomaly was 1.13 °C above the 1964–1993 mean, twice the interannual variability. The temperature extremes set the highest records in T_{XX} and T_{Nx} during summer 2015 and were about three times the interannual variability. The extreme hot summer in 2015 occurred in the context of steadily increasing temperatures in recent decades.

2) It is estimated that about 65–72% of the observed area-averaged summer mean changes in the SAT, T_{max} and T_{min} over western China in 2015 resulted from changes in boundary forcings, including the SST/SIE and anthropogenic forcing. The magnitude of the area-averaged T_{XX} and T_{Nx} in the model responses to changes in all forcings is about 30.2% (35.7%) of the observed increase in T_{XX} (T_{Nx}). The model results indicate that the internal variability of the atmosphere might play a part in the severity of the observed seasonal mean changes in the SAT, T_{max} , T_{min} and hot temperature extremes over western China in 2015.

3) The changes in anthropogenic forcing resulted in about 42% of the simulated warming of the SAT, about 40% of the increase in simulated daytime temperature extremes (T_{XX} and T_{max}) and about 60% of the increase in the simulated night-time temperature extremes (T_{Nx} and T_{min}), suggesting an important role for recent changes in anthropogenic forcing in the severity of hot extremes in western China, particularly night-time extremes. In general, the emissions of GHG and AA both make a positive contribution to the warming of SATs and increases in temperature extremes, although the effects of changes in forcing by GHG are stronger. The increase in the summer

mean SAT and temperature extremes in response to changes in AA emissions are probably the result of the downstream extension of the climate response to reduced emissions of AA over Europe.

4) The changes in the SST/SIE explain the additional signals in the simulation. The SST changes over the Pacific Ocean, where a super El Niño event was developing, had a dominant role in the response to changes in the SST/SIE. The strong warm SST over the central and eastern tropical Pacific Ocean led to positive anomalies in atmospheric thickness around the tropical and subtropical regions, including the southern part of western China, as a Kelvin wave response. The positive thickness anomalies were related to an anticyclonic circulation anomaly, which favoured an increase in downward solar radiation and therefore contributed to the severity of the hot extremes, particularly to the severity of the daytime extremes (T_{xx} and T_{max}).

The simulations indicate that the severity of the extreme hot summer over western China in 2015 was caused by a combination of forced responses and the internal variability of the atmosphere. In addition to tropical forcing, the extreme high temperatures over western China in 2015 were related to a Rossby wave pattern over mid-latitudes extending from the North Atlantic to East Asia. This mid-latitude wave pattern, probably caused by the internal variability of the atmosphere (e.g., Sato et al. 2003, 2006; Kosaka et al. 2009), resulted in an anticyclonic circulation over western China that warmed the surface through increased downward solar radiation and the

anomalous sinking of an air mass. Thus the observed warming and increase in hot extremes that is not explained by all forcing changes may result from the internal variability of the atmosphere, principally through the mid-latitude Rossby wave pattern.

This study detected the forcing response in the severity of SAT warming and increase in temperature extremes over western China in summer 2015. In addition to the changes in the SST/SIE, the changes in anthropogenic forcing set the conditions for the severity of the extreme hot summer in western China in 2015. It should be noted that this study focused on understanding the severity of the extreme hot event over western China in 2015. It differs from previous attribution studies focusing on the risk of occurrence of this event (Miao et al., 2016; Sun et al., 2016). Our results suggest a role for anthropogenic forcing in the severity of this event, while previous studies have argued that the increase in the risk of this kind of hot event can be attributed to human influences. Different aspects of the attribution of the 2015 extreme hot event are addressed in our study. Our conclusions are based on the study of one model and the quantitative partitioning of causes could be potentially sensitive to model bias. However, we are confident that our main results are realistic given the model's ability to reproduce the magnitude and spatial characteristics of this extreme temperature event.

Acknowledgements. This study was supported by the National Natural Science Foundation of China under Grants 416750788, U1502233, 41320104007, by the

405 Youth Innovation Promotion Association of the Chinese Academy of Sciences (No.
406 2018102) and by the UK–China Research & Innovation Partnership Fund through the
407 Met Office Climate Science for Service Partnership China as part of the Newton Fund.
408 BD was supported by the Natural Environment Research Council via the National
409 Centre for Atmospheric Science. The authors thank the two anonymous reviewers for
410 their constructive comments and suggestions on the earlier version of this paper.

References

- Bindoff, N. L., et al., 2013: *Detection and attribution of climate change: from global to regional*. The physical science basis Contribution of working group I to the fifth assessment report of the intergovernmental panel on climate change, Stocker, T. F., et al., Eds., Cambridge University Press, Cambridge, UK, 867–952.
- CMA, 2016: *China Climate Bulletin 2015*. China Meteorological Administration, 50 pp. (in Chinese)
- Cattiaux, J., H. Douville, R. Schoetter, S. Parey, and P. Yiou, 2015: Projected increase in diurnal and interdiurnal variations of European summer temperatures. *Geophys. Res. Lett.*, **42**, 899–907.
- Christidis, N., P. A. Stott, and S. J. Brown, 2011: The role of human activity in the recent warming of extremely warm daytime temperatures. *J. Climate*, **24**, 1922–1930.
- Díaz, J., R. García, F. V. de Castro, E. Hernandez, C. Lopez, and A. Otero, 2002: Effects of extremely hot days on people older than 65 years in Seville (Spain) from 1986 to 1997. *Int. of Biometeorol.*, **46**, 145–149.
- Dole, R., et al., 2011: Was there a basis for anticipating the 2010 Russian heat wave? *Geophys. Res. Lett.*, **38**, L06702.
- Dong, B. -W., R. T. Sutton, L. Shaffrey, L. Wilcox, 2016a: The 2015 European heat wave. *Bull. Amer. Meteorol. Soc.*, **97**, S5–S10, doi:

- 10.1175/BAMS-D-16-0140.1.
- Dong, B.-W., R. T. Sutton, W. Chen, X. D. Liu, R. Y. Lu, and Y. Sun. 2016b: Abrupt summer warming and changes in temperature extremes over Northeast Asia since the mid-1990s: Drivers and physical processes. *Adv. Atmos. Sci.*, **33**, 1005–1023, doi: 10.1007/s00376-016-5247-3.
- Hewitt, H. T., D. Copsey, I. D. Culverwell, et al., 2011: Design and implementation of the infrastructure of HadGEM3: The next-generation Met Office climate modelling system. *Geoscientific Model Development*, **4**, 223–253, doi:10.5194/gmd-4-223-2011.
- Kilbourne, E. M., 1997: Heat Waves and Hot Environments. In *The Public Health Consequences of Disasters*. In: Noji E K, eds. New York: Oxford University Press. pp245–269.
- King, A. D, G. J. van Oldenborgh, D. J. Karoly, et al., 2015: Attribution of the record high Central England temperature of 2014 to anthropogenic influences. *Environ. Res. Lett.*, **10**, 054002.
- King, A. D., M .T. Black, S. -K. Min, et al., 2016: Emergence of heat extremes attributable to anthropogenic influences. *Geophys. Res. Lett.*, doi:10.1002/2015GL067448.
- Kosaka, Y., H. Nakamura, M. Watanabe, and M. Kimoto, 2009: Analysis on the dynamics of a wave-like teleconnection pattern along the summertime Asian jet based on a reanalysis dataset and climate model simulations. *J. Meteor. Soc.*

- 453 *Japan*, **87**, 561–580, doi:10.2151/jmsj.87.561.
- 454 Kysely, J., and E. Plavcova, 2012: Biases in the diurnal temperature range in Central
455 Europe in an ensemble of regional climate models and their possible causes.
456 *Climate Dyn.*, **39**, 1275–1286.
- 457 Lamarque, J. F., et al., 2010: Historical (1850–2000) gridded anthropogenic and
458 biomass burning emissions of reactive gases and aerosols: Methodology and
459 application. *Atmos. Chem. Phys.*, **10**, 7017–7039.
- 460 Lamarque, J. F., et al., 2011: Global and regional evolution of short-lived
461 radiatively-active gases and aerosols in the Representative Concentration
462 Pathways. *Climatic Change*, **109**, 191–212.
- 463 Ma, S. M., T. J. Zhou, D. Stone D, et al., 2017: Attribution of the July-August 2013
464 Heat Event in Central and Eastern China to Anthropogenic Greenhouse Gas
465 Emissions. *Environ. Res. Lett.*, **12**, 054020.
- 466 Miao, C., Q. Sun, D. Kong, and Q. Duan, 2016: Record-Breaking Heat in Northwest
467 China in July 2015: Analysis of the Severity and Underlying Causes. *Bull. Amer.*
468 *Meteor. Soc.*, **97**, S97–S101.
- 469 Otto, F. E. L., et al., 2012: Reconciling two approaches to attribution of the 2010
470 Russian heat wave. *Geophys. Res. Lett.*, **39**, L04702.
- 471 Rahmstorf, S., and D. Coumou, et al., 2011: Increase of extreme events in a warming
472 world. *Proc. Natl. Acad. Sci.*, **108**, 17905–17909.
- 473 Rayner, N. A., et al., 2003: Global analyses of sea surface temperature, sea ice, and

- 474 night marine air temperature since the late nineteenth century. *J. Geophys. Res.*,
475 **108**, 4407
- 476 Sato, N., and M. Takahashi, 2003: Formation mechanism of vorticity anomalies on the
477 subtropical jet in the midsummer northern hemisphere. *Theoretical and Applied*
478 *Mechanics Japan*, **52**, 109–115, doi:10.11345/nctam.52.109.
- 479 Sato, N., and M. Takahashi, 2006: Dynamical processes related to the appearance of
480 quasi-stationary waves on the subtropical jet in the midsummer northern
481 hemisphere. *J. Climate*, **19**, 1531–1544, doi:10.1175/JCLI3697.1.
- 482 Seneviratne, S. I., et al., 2012: Changes in climate extremes and their impacts on the
483 natural physical environment. In: Field CB et al., eds. Managing the risks of
484 extreme events and disasters to advance climate change adaptation. A special
485 report of working groups I and II of the IPCC. Cambridge: Cambridge
486 University Press.
- 487 Stott, P. A., et al., 2013: Attribution of Weather and Climate-Related Events. In: Asrar
488 G, Hurrell J, eds. Climate Science for Serving Society.
- 489 Stott, P. A., 2016: How climate change affects extreme weather events. *Science*, **352**,
490 1517–1518.
- 491 Sun, Y., L. C. Song, H. Yin, et al., 2016: Human Influence on the 2015 extreme high
492 temperature events in western China. *Bull. Amer. Meteorol. Soc.*, **97**, S5–S9.
- 493 WMO, 2015: The state of greenhouse gases in the atmosphere based on global
494 observations through 2014. WMO Greenhouse Gas Bull. No. 11 4 pp.

- 495 WMO Press Conference, 2015: Status of the global climate in 2015 Geneva, 25
496 November 2015. [Available online at
497 [http://webtv.un.org/meetings-events/watch/wmo-press-conference-status-of-the-](http://webtv.un.org/meetings-events/watch/wmo-press-conference-status-of-the-global-climate-in-2015-geneva-25-november-2015/4631098881001#full-text)
498 [global-climate-in-2015-geneva-25-november-2015/4631098881001#full-text](http://webtv.un.org/meetings-events/watch/wmo-press-conference-status-of-the-global-climate-in-2015-geneva-25-november-2015/4631098881001#full-text)].
499 [Accessing data: November 25, 2015].
- 500 Xinhua net, 2015. Feel the “fire Island” Turpan extreme high temperature 24 July
501 2015. [Available online at
502 http://news.xinhuanet.com/politics/2015-07/24/c_128057198.html]. [Accessing
503 data: July 24, 2015].
- 504 Zwiers, F. W., X. B. Zhang, and Y. Feng, 2011: Anthropogenic influence on long
505 return period daily temperature extremes at regional scales. *J. Climate*, **24**,
506 296–307
- 507 Zhou, B. T., Y. Xu, J. Wu, S.Y. Dong, and Y. Shi, 2016: Changes in temperature and
508 precipitation extreme indices over China: analysis of a high-resolution grid
509 dataset. *Int. J. Climatol.*, **36**, 1051–1066.